PHYSICAL REVIEW A VOLUME 34, NUMBER 3 SEPTEMBER 1986

Electron mobility in liquid krypton as function of density, temperature, and electric field strength

Finn M. Jacobsen,* Norman Gee, and Gordon R. Freeman
Department of Chemistry, University of Alberta, Edmonton, Alberta, Canada T6G 2G2

(Received 14 April 1986)

The electron mobility μ was measured in liquid Kr at $95\times10^{26}\leq n\leq172\times10^{26}$ molecules/m^3, and $121\leq T\leq206$ K. At low fields a field-independent $\mu=\mu_0$ was obtained at each density. The density dependence of μ_0 is compared to that predicted by the deformation potential theory of Basak and Cohen; μ_0 is maximum at $(13.7\pm0.4)\times10^{27}$ molecules/m^3. Scattering lengths were calculated for both liquid Kr and Xe, and their density dependence was examined using the recent model of Baird [Phys. Rev. A 32, 1235 (1985)]. At higher fields, μ is field dependent. The effect of density on the field dependence is examined.

I. INTRODUCTION

Theoretical investigations into the electronic states of simple liquids are connected to experiment by the low-field, thermal mobility μ_0 of extra electrons in argon, krypton, and xenon.[1-11] Values of μ_0, which are the constant values of the mobility μ at electric fields E less than some threshold value E^{th}, have been reported for the entire liquid ranges of argon[12,13] and xenon,[8,14] so comparison to theory can be effected.[1,2,4,8-10] Such is not the case for krypton: (a) At $T<120$ K, μ might be field dependent at the field strengths $>2\times10^3$ V m^{-1} used;[15,16] (b) in the main temperature study μ was field dependent.[17] Values of μ_0 in liquid Kr would complete the important series Ar, Kr, and Xe. Furthermore, the generality of empirical relations obtained from comparing Ar to Xe results, such as the maximum in μ_0 occurring at the same density $n=1.2\times10^{28}$ molecules/m^3,[13] could be tested. This work reports values of μ at low and intermediate fields, and at $121.3\leq T\leq205.8$ K in liquid Kr.

II. EXPERIMENTAL

A. Material

Matheson research-grade krypton (>99.995%) was further purified in a grease-free vacuum line by passage through a quartz U tube filled with clean copper pellets at 773 K, bubbling at room temperature through a sodium-potassium alloy, and holding on potassium mirrors in 0.002 m^3 glass bulbs at a pressure of 0.2 MPa for >2 months prior to use.

B. Equipment and techniques

The two high-pressure conductance cells used were like that in Ref. 18. The drift distance l was measured with precision calipers to be 3.15 and 3.23 mm, respectively. Other experimental details are in or cited in Ref. 19. The Cu-constantan thermocouples used to monitor the temperature at the top, middle, and bottom of the cells had been calibrated in combination with the Fluke 2100A digital thermometer, using liquid nitrogen at 92 kPa (76.7 K), and slush baths of iso-octane (165.8 K), octane (216.4 K), acetone (177.8 K), carbon tetrachloride (250.2 K), and ice water (273.2 K). Temperature differences on the cell body were ≤0.4 K.

The electrons were generated with x rays formed by directing a 10-nsec pulse of 1.7-MeV electrons into a 3-mm-thick gold target. The sample dose was $\sim9\times10^7$ eV/g.

The mobility was determined from the time of flight t_d:

$$\mu=l^2/Vt_d\ , \qquad (1)$$

where V is the applied voltage. The average of a positive and a negative polarity measurement, applied to check for strain voltages in the cell, was used.

The collection time τ of the electrons is several orders of magnitude shorter than that, τ_+, of the concurrently generated cations. As the electrons are swept from the cell the cations are left behind so the space acquires a net charge. If the number of charges is great enough the field that they produce counteracts an appreciable fraction of the applied field, and τ becomes larger than the unperturbed t_d. Furthermore, ion-electron neutralization might occur to an appreciable extent during τ. These two effects are discussed in the Appendix. The net correction factor f_{sr} for space charge (s) and homogeneous recombination (r) is

$$\begin{aligned} f_{\text{sr}}&=t_d/\tau\\ &=2B/\ln[(1+B)/(1-B)]\ , \end{aligned} \qquad (2)$$

where

$$B=l(e\langle n_+\rangle/2\epsilon_0\epsilon V)^{1/2}\ , \qquad (3)$$

where e is the electron charge, $\langle n_+\rangle$ is the average number density of cations during τ, ϵ_0 is the permittivity of vacuum, and ϵ is the dielectric constant of the fluid. In the limit $\langle n_+\rangle\rightarrow0$, $f_{\text{sr}}=1$ and $t_d=\tau$.

The lowest voltage used was 5 V and $\langle n_+\rangle$ was in the vicinity of 10^{13} ions/m^3 ($\sim10^7$ ions in the collection volume). The radiation pulse dose changed from month to month, so at 5 V the value of f_{sr} was 1.00 for the samples at 206 and 201 K, 1.03 at 192 K, 1.05 at 121, 145, and 185 K, and 1.13 at 170 K. The factor $(1-f_{sr})$ decreased approximately as $V^{-1/2}$ in a given sample under these conditions.

C. Physical properties

Values of the densities were obtained from Refs. 20 and 21, compressibilities from Refs. 20 and 22, and sound velocities from Refs. 22 and 23. The liquids were under their vapor pressure, so T and n changed concomitantly.

III. RESULTS

A. Electric field effect

Electron mobilities were measured in liquid krypton at seven densities from 95 to 172 (10^{26} molecules/m^3) (Table I). Five of the data sets are shown in Fig. 1 along with available values from the literature. Mobilities from Refs. 15 and 16 at near 172×10^{26} molecules/m^3 reached the low-field, thermal-electron region, although they did not by themselves show a constant μ at low fields. The krypton of Ref. 16 apparently contained a small amount of nitrogen, because the low-field μ is lower and the high-field μ higher than those from Ref. 15. This is characteristic of a stronger scatterer impurity in a noble liquid.[13]

At all densities $n\geq120\times10^{26}$ molecules/m^3, μ decreases at $E\gtrsim4$ kV/m (Fig. 1). At a density between 120 and 108 (10^{26} molecules/m^3) the sign of the initial field effect changes. At the latter density μ initially increases with E at intermediate fields, reaches a maximum μ_{max} at $E\approx23$ kV/m, then decreases at higher fields (Fig. 1). Values of the low-field limit μ_0 and of the threshold field E^{th} for field dependence are listed in Table I along with relevant physical properties. Values of E^{th} were chosen where μ differed from μ_0 by 5%.

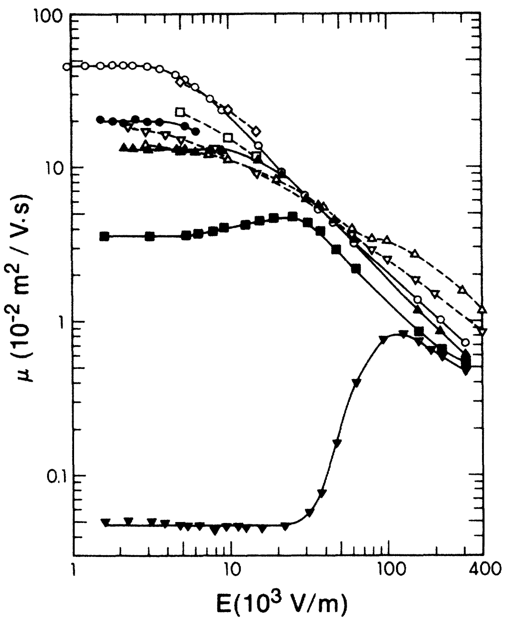

FIG. 1. Field-strength dependence of electron mobility in liquid krypton at (n (10^{26} molecules/m^3), $T(K)$): ● (172,121.3); ○ (141,170.1); ▲ (120,191.6); ■ (108,200.1); ▼ (95,205.8); ▽, Ref. 15 (176,117); △, Ref. 16 (174,120); □, Ref. 17 (154,152); ◇, Ref. 17 (135,180). The lines are visual guides.

B. Comparison with xenon and argon

Values of μ in xenon at different n and T are not easily read from Ref. 14. The values of μ_0, n,[24] and T used in

TABLE I. Data for liquid krypton.

T (K)	n[a] (10^{26} molecules/m^3)	μ_0[b] (10^{-4} m^2/V s)	μ_{max}[c] (10^{-4} m^2/V s)	χ_T[d] (10^{-9} m^2/N)	χ_S[e] (10^{-9} m^2/N)	c_0[f] (m/s)	E^{th} (10^3 V/m)	$\frac{v_d^{th}}{c_0}$	v_{sat}[g] (m/s)
113	204[h]	3700[h,i]	3700	0.8	0.91[j]	1100[i]	4.0[i]	1.3	8800[i]
117	175	1800[i]	1800	1.7	0.86	696	4.5[i]	1.2	3800[i]
121.3	172	1980±40	1980	1.86	0.91	679	4.9	1.4	
145.3	158	2510±80	2510	3.27	1.36	576	3.5	1.4	
170.1	141	4630±20	4630	7.40	2.47	454	3.7	3.6	2200
185.4	127	2530±40	2530	16.6	4.29	364	5.6	3.7	
191.6	120	1300±20	1300	24.3	5.72	321	11	4.2	2000
200.1	108	357±3	470	60.1	10.9[k]	247[l]	7.0	1.1	1400
205.8	95	4.7±0.2	82		21.9[k]	186[l]	26	0.06	~1200
300	0.0050[m]	264 000[m]	720 000[m]	480 000[n]	290 000[j]	223[o]	0.0039[m]	0.5	1200[m]

[a] References 20(a) and 21.
[b] Thermal-electron mobility, $E\rightarrow0$.
[c] Maximum mobility in plot of μ against E.
[d] Reference 20.
[e] References 20 and 22.
[f] Reference 22.
[g] ±100 m/s.
[h] Solid.
[i] Reference 15.
[j] Calculated from n and c_0.
[k] Calculated from Ref. 23(a) c_0 values.
[l] Reference 23.
[m] Low-density gas, Ref. 28.
[n] Low-density limit equals $1/nk_BT$.
[o] $(\gamma k_BT/M)^{1/2}$, Ref. 29.

preparing graphs in Ref. 14 are listed in Table II.

In low-density xenon[14] and argon[13] there is a hump in the plots of μ against E, as in low-density krypton (Fig. 1). In krypton this hump disappears at $n=11\times10^{27}$ molecules/m^3 whereas in both argon and xenon it disappeared at $n=10\times10^{27}$ molecules/m^3.[13] The values of $\mu_{\max}$ in Tables I and II refer to the maximum value of μ at that density, at whatever field strength μ is maximum.

In plots of μ_0 against density there is a maximum, designated $\mu_0^{\max}$. The density at which $\mu_0^{\max}$ occurs is between 13 and 14 (10^{27} molecules/m^3) in krypton (Table I), but it occurs at 12×10^{27} molecules/m^3 in both xenon and argon.[13] It has been noted[25] that in a corresponding states plot, $n(\mu_0^{\max})/n_c$, where n_c is the density of the critical fluid, is in the order $\mathrm{Ar}<\mathrm{Kr}<\mathrm{Xe}$, which is in the same order as the polarizabilities.

IV. DISCUSSION

A. Threshold field for electron heating, and saturation drift velocity

At $E<E^{\mathrm{th}}$ the electrons are near thermal equilibrium with the fluid, and $\mu=\mu_0$. At $E>E^{\mathrm{th}}$ the electrons gain more energy from the field than they lose in collisions with the molecules, so the average electron energy increases above thermal. The Shockley model for electron heating indicates that in a simple solid or liquid electron heating should become appreciable when the drift velocity is near the speed of sound c_0 in the material.[4,15] Thus one expects

$$v_d^{\mathrm{th}}/c_0\approx1\ , \qquad (4)$$

where

$$v_d^{\mathrm{th}}\approx\mu_0E^{\mathrm{th}}\ . \qquad (5)$$

In krypton at $n\geq158\times10^{26}$ molecules/m^3, $n/n_c\geq2.4$, approximation (4) is true (Table I). It is also true in argon[13] and xenon[14] at corresponding densities.

In the low-density-gases approximation (4) is also expected to apply.[26,27] In krypton $v_d^{\mathrm{th}}/c_0=0.5$ (Table I, data from Refs. 28 and 29), the same as in argon[13] and xenon.[14]

In liquid krypton at $120\leq n/10^{26}\leq141$, the apparent value of v_d^{th}/c_0 is much greater than unity (Table I). The ratio increases to a cusp at the density where $d\mu/dE$ changes sign.[25,30] At these densities the mobility is nearly independent of electron energy in the near thermal region, and electron heating is quite extensive before μ changes by 5%; hence the true E^{th} is much lower than the selected value.

The apparent low value at 95×10^{26} molecules/m^3 ($T/T_c=0.98$) is due to the decrease of μ_0 by formation of quasilocalized states of the electrons in density fluctuations in the near critical liquid. The electrons are not quasifree, as required by approximation (4). Similar behavior is observed in argon and xenon.[13,14,25]

At intermediate fields the drift velocity tends toward a plateau (Fig. 2). The "saturation" values v_{sat} are listed in Table I and compared with those in argon[13,15,28] and xenon[14,15] in Fig. 3. In the low-density gases v_{sat} is similar in the three gases, being 1000 m/s in argon and xenon, and 1200 m/s in krypton. With increasing density there is a gradual decrease of v_{sat} in argon and a gradual increase in xenon. In krypton v_{sat} remains constant up to

TABLE II. Electron mobility[a] and scattering length in Xe.

T (K)	n[b] (10^{27} molecules/m^3)	μ_0 (10^{-4} m^2/V s)	$\mu_{\max}$ (10^{-4} m^2/V s)	ϵ[c]	χ_T[d] (10^{-9} m^2/N)	χ_S[e] (10^{-9} m^2/N)	a_T[f] (10^{-10} m)	a_S[g] (10^{-10} m)	a_{liq}[h] (10^{-10} m)
163	14.1	1700	1700		1.61	0.80	0.37	0.50	0.26
188	13.3	2480	2480	1.908	2.40	1.09	0.23	0.34	0.17
209	12.6	3730	3730	1.847	3.57	1.46	0.15	0.23	0.08
216	12.3	4500	4500	1.821	4.13	1.63	0.12	0.20	0.04
219	12.2	4600	4600	1.813	4.44	1.71	0.12	0.19	0.02
223	12.0	6000	6000	1.796	4.87	1.83	−0.10[i]	−0.16[i]	−0.002
234	11.5	4400	4400	1.754	6.53	2.28	−0.10	−0.17	−0.08
261	10.0	750	750	1.635	18.1	4.67	−0.16	−0.31	−0.32
278	8.6	163	302[j]	1.530	57	10.5[k]	−0.21	−0.49	−0.59
288	6.8	54	144[j]	1.404		37.0[k]		−0.55	−1.0
$290=T_c$	5.0	3.0	46[j]	1.287	∞	144.0[k]	0	−1.6	−1.5

[a] Values used in, but not listed in, Ref. 14.

[b] Reference 24.

[c] Dielectric constant calculated from Clausius-Mosotti equation, using liquid-phase Clausius-Mosotti function from Ref. 35.

[d] Reference 20(b).

[e] References 20(b) and 22.

[f] Equation (6) using measured μ_0 and $S(0)$ instead of $S(k)$.

[g] Equation (6) using measured μ_0.

[h] Baird's model (Ref. 33), Eqs. (6)–(9) (see text).

[i] Sign of scattering length chosen to conform with model (Ref. 33).

[j] Peak of μ against E plot.

[k] Calculated using Ref. 23 c_0 values.

beyond the critical density, so the behavior is intermediate between those in argon and xenon. However, at higher densities v_{sat} increases in both krypton and argon.

In all three gases at densities up to the critical the value of v_{sat} varied by only 10% or less (Fig. 3). The cause of v_d becoming nearly independent of E is electron heating and the rapid increase of the momentum transfer cross section at energies higher than that of the Ramsauer-Townsend scattering minimum.[14,31]

The increase of v_{sat} with density in the dense liquids and solids (Fig. 3) is attributed to two factors:[14] (a) diffraction effects, as the disorder decreases due to spatial restriction; (b) lowering the mean energy of the electrons by inelastic scattering, involving electrical anisotropies created by intermolecular collisions. A quantitative model is lacking.

The decrease of v_{sat} in argon at intermediate densities is attributed to the relatively hard nature of the electron-argon multibody interactions[32] in the highly disordered fluid.

B. Density dependence of μ_0

The variation of μ_0 with n in the noble liquids is often interpreted in terms of the deformation potential theory.[4] The thermal electron moves in an otherwise empty conduction band, undergoing scattering by potentials created by local fluctuations in molecular density.

Mobilities calculated from deformation potentials,[9] using measured energies of the quasifree electron state, are compared with experimental values in Fig. 4. The calculated mobility maximum is about half of the observed value and occurs at a density 10% lower than observed. The calculated decrease of μ_0 on the high-density side of $\mu_0^{\max}$ is about sixfold greater than observed. The calculated peak is much too narrow.

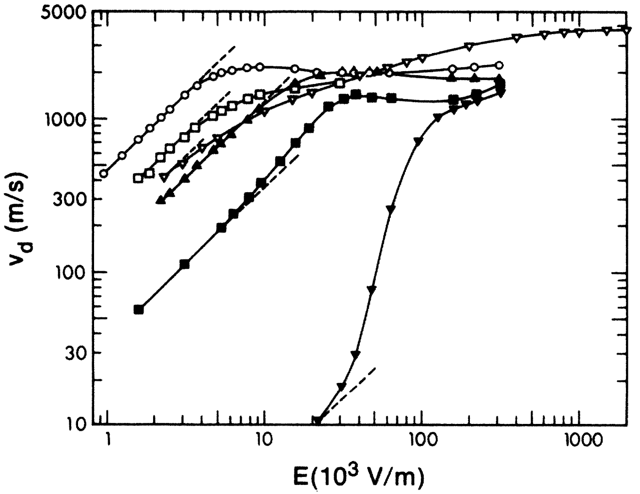

FIG. 2. Field dependence of electron drift velocity in liquid Kr. Symbols as Fig. 1, except □ is 159×10^{26} molecules/m^3, 145.3 K. The dashed lines indicate a slope of 1, and extend from the low-field region where μ_0 was determined.

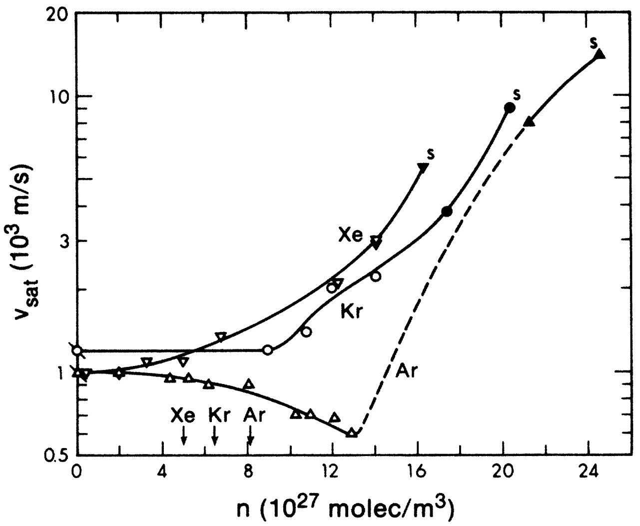

FIG. 3. Saturation drift velocities, from plateau values as in Fig. 2, as functions of density. Argon: △ (Ref. 13), ⟍△ (Ref. 28), ▲ (Ref. 15). Krypton: ○ (Table I), ⟍○ (Ref. 28), ● (Ref. 15). Xenon: ▽ (Ref. 14), ▼ (Ref. 15). The arrows indicate n_c. The highest point on each curve labeled S represents the solid near the triple point.

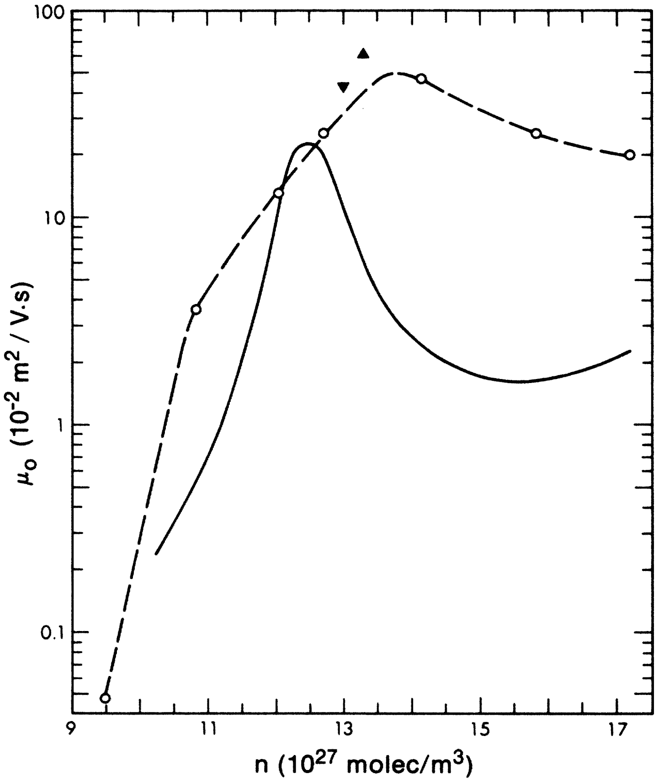

FIG. 4. Density dependence of thermal-electron mobility in liquid krypton. Experimental, ○. Calculated: The solid line shows the deformation potential theory (Ref. 9); ▼ [Ref. 1(b)], ▲ (Ref. 13), scattering-length theory.

A closer estimate of $\mu_0^{\max}$ was obtained using the zero-scattering-length model[1(b),13] (Fig. 4). However, the latter model requires input of the density at which $\mu_0^{\max}$ occurs.

Recently the electron scattering-length model was extended by Baird to interpret the density dependence of μ_0 in liquid argon.[33] The value of the scattering-length a_S was obtained from the experimental μ_0, using Lekner's modification of the Lorentz equation:[1]

$$\mu_0 = \frac{2}{3}\left[\frac{2}{\pi m k_B T}\right]^{1/2} \frac{e}{4\pi a_S^2 n S(k)} , \tag{6}$$

where m is the mass of the electron, k_B is Boltzmann's constant, $S(k) = nk_B T \chi_S$ is the structure factor, and χ_S is the adiabatic compressibility of the fluid. This value of a_S was compared to a value a_{liq} calculated from that in the gas phase, a_{gas}:

$$a_{\text{liq}} = a_{\text{gas}} f_1 , \tag{7}$$

where f_1 is a screening function,

$$f_1(u_1,\epsilon) = \left[\frac{1}{u_1 \epsilon}\right] \frac{u_1(\epsilon+2)-(\epsilon-1)}{(2\epsilon+1)-2u_1(\epsilon-1)} , \tag{8}$$

where

$$u_1 = \alpha / 4\pi\epsilon_0 r^3 , \tag{9}$$

where α is the dipole polarizability in SI units of C m^2/V, and r is the cavity radius from the Böttcher-Onsager equation.[34] Baird used $a_{\text{gas}} = -8.7 \times 10^{-11}$ m and $u_1 = 0.083$ for argon and found that a_{liq} had the same density dependence as a calculated from μ_0. He found that f_1 goes to zero at the density of $\mu_0^{\max}$, at which point μ_0 becomes limited by density fluctuations or higher-order electrostatic interactions.

Baird's model was applied to electrons in krypton and xenon. Values of the dielectric constant were calculated from the Clausius-Mosotti equation; the molar polarization is 6.45 cm^3/mol for liquid krypton and 10.52 cm^3/mol for liquid xenon.[35] Values of a_{gas} are -1.96×10^{-10} m for krypton and -3.44×10^{-10} m for xenon.[36] The value of u_1 was selected so a_{liq} would go through zero at the density of $\mu_0^{\max}$; $u_1 = 0.15$ for krypton and 0.22 for xenon, compared to 0.083 for argon.[33] The values of a_{liq} so obtained are compared in Tables II and III with values of a_s calculated from Eq. (6). The agreement is reasonable at low densities, but less satisfactory at high densities.

Sometimes the $k=0$ structure factor $S(0)$ is used in Eq. (6);[1(a)] $S(0) = nk_B T \chi_T$, where χ_T is the isothermal compressibility of the liquid. Substitution of $S(0)$ for $S(k)$ in Eq. (6) gives a_T, which is closer to the a_{liq} values in the dense liquids (Tables II and III).

ACKNOWLEDGMENTS

We are grateful to the Natural Sciences and Engineering Research Council of Canada for financial assistance, and to the staff of the Radiation Research Center for assistance with the electronic equipment.

APPENDIX

Space charge during collection of the electrons can make $\tau > t_d$ and $f_{\text{sr}} > 1.0$. Equation (2) is obtained by considering the effect of space charge on τ. Homogeneous neutralization decreases density of cations n_+, thereby decreasing the space charge.

1. Space charge without homogeneous recombination

At time $t=0$, $n_+ = n_e = n_0$, where n_e is the electron number density and n_0 the initial ion-pair density. At a later time t some electrons have been collected at the anode. The situation is depicted in Fig. 5. As $\tau \ll \tau_+$, n_+ still equals n_0 at $0 < x \le x_0$, but $n_e = 0$. The effect of the excess cations at 0 to x_0 is to counteract part of the applied field and increase τ. The field acting on the electrons at $x_0 < x < l$ is $E(x_0)$. Solving Gauss's equation[37] for Fig. 5 gives

TABLE III. Scattering lengths in liquid Kr.

T (K)	ϵ[a]	a_T[b] (10^{-10} m)	a_S[c] (10^{-10} m)	a_{liq}[d] (10^{-10} m)
121.3	1.678	0.31	0.44	0.23
145.3	1.612	0.20	0.30	0.14
170.1	1.535	0.10	0.17	0.01
185.4	1.473	−0.09[e]	−0.18[e]	−0.11
191.6	1.444	−0.11	−0.22	−0.18
200.1	1.394	−0.14	−0.33	−0.29
205.8	1.340		−2.2	−0.44

[a] Calculated from Clausius-Mossoti equation using liquid-phase Clausius-Mossoti function from Ref. 35.

[b] Equation (6) using experimental μ_0 and $S(0)$ instead of $S(k)$.

[c] Equation (6) using experimental μ_0.

[d] Baird's model (Ref. 33), Eqs. (6)–(9) (see text).

[e] The model (Ref. 33) indicates that these are negative.

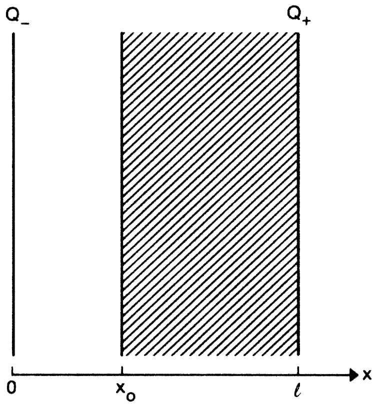

FIG. 5. Schematic of charge distribution in cell at time t. Q_- and Q_+ are the total charge on negative and positive electrodes due to voltage V. At $0<x\le x_0$, $n_+=n_0$ and $n_e=0$. At $x_0<x<l$, $n_+=n_0=n_e$.

$$E(x)=\frac{1}{\epsilon\epsilon_0}\frac{Q_-}{A}+\frac{1}{\epsilon\epsilon_0}\int_0^x n_+e\,dx$$

$$=\begin{cases}\dfrac{1}{\epsilon\epsilon_0}\left[\dfrac{Q_-}{A}+n_+e\right], & 0\le x\le x_0\\ E(x_0)\ , & x_0<x<l\end{cases} \tag{A1}$$

where A is the area of the collecting electrode and Q_- is the charge on the electrode. The voltage drop V across the gap equals

$$V=-\int_0^l E(x)dx\ . \tag{A2}$$

The results of Eq. (A2) can be rearranged to give

$$\frac{Q_-}{A\epsilon\epsilon_0}=-\frac{V}{l}+\frac{1}{2}\frac{en_+x_0^2}{\epsilon\epsilon_0 l}-\frac{en_+x_0}{\epsilon\epsilon_0} \tag{A3}$$

so

$$E(x_0)=-\frac{V}{l}+\frac{1}{2}\frac{en_+x_0^2}{\epsilon\epsilon_0 l}\ . \tag{A4}$$

The measured drift velocity at x_0, $v_d(x_0)$, equals $dx_0/dt=-\mu E(x_0)$ so

$$-dx_0/dt=\frac{\mu V}{l}\left[1-\frac{en_+x_0^2}{2\epsilon\epsilon_0}\right], \tag{A5}$$

$$\int_0^l\frac{dx_0}{1-\dfrac{en_+x_0^2}{2\epsilon\epsilon_0 V}}=\frac{l}{t_d}\int_0^\tau dt\ , \tag{A6}$$

where t_d is the time of flight and equals τ if the space charge is negligible. Substituting

$$z=(en_+/2\epsilon\epsilon_0 V)^{1/2} \tag{A7}$$

in Eq. (A6) gives

$$t_d=\tau\{2lz/\ln[(1+lz)/(1-lz)]\}$$

$$=\tau f_s\ , \tag{A8}$$

where f_s is the space-charge correction. In the limit $n_+\to 0$, $\ln[(1+lz)/(1-lz)]\sim\ln(1+2lz)\sim 2lz$, so $f_s\sim 1$ and $t_d\sim\tau$.

2. Space charge with homogeneous recombination

Homogeneous recombination decreases n_+ and reduces f_s. In the reaction zone $x_0\le x<l$, $n_+=n_e=n$, and recombination is second order:

$$\frac{dn_+(t)}{dt}=-k_2n^2\ , \tag{A9}$$

where k_2 is the second-order rate constant. Integration of Eq. (A9) between the limits $n=n_0$ at $t=0$ and $n=n_+(t)$ at $t=t$ gives $n_+(t)^{-1}+n_0^{-1}=k_2t$ or

$$n_+(t)=\frac{n_0}{1+n_0k_2t}\ . \tag{A10}$$

We use for n_+ in Eq. (A7) an average density:

$$\langle n_+\rangle=\frac{1}{\tau}\int_0^\tau n_+(t)dt \tag{A11}$$

to account for homogeneous recombination. From Eqs. (A10) and (A11),

$$\frac{\langle n_+\rangle}{n_0}=\frac{1}{j}\ln(1+j)\ , \tag{A12}$$

where $j=k_2n_0\tau$. The ratio $\langle n_+\rangle/n_0$ can be obtained by experimentally measuring $q(\tau)/q(0)$, where $q(0)$ is the total collected electron charge. In the presence of a loss process,[19]

$$\frac{q(\tau)}{q(0)}=\frac{2}{j}[(1+j^{-1})\ln(1+j)-1]\ . \tag{A13}$$

The experimental $q(\tau)/q(0)$ gives a value of j, which then gives $\langle n_+\rangle/n_0$ by Eq. (A12). We found that the high-field limit for q was reached at 1000 V. The correction factor $f_{\rm sr}$ is obtained using $\langle n_+\rangle$ instead of n_+ in Eq. (A7):

$$f_{\rm sr}=2B/\ln[(1+B)/(1-B)]\ , \tag{A14}$$

where $B=l(e\langle n_+\rangle/2\epsilon_0\epsilon V)^{1/2}$.

---

[*] Present address: Department of Physics and Astronomy, University College London, Gower Street, London WC1E 6BT, England, United Kingdom.

[1] (a) J. Lekner, Phys. Rev. **158**, 130 (1967); (b) Phys. Lett. **27A**, 341 (1968).

[2] J. A. Jahnke, N. A. Holzworth, and S. A. Rice, Phys. Rev. A **5**, 463 (1972).

[3] J. Lekner and A. R. Bishop, Philos. Mag. **27**, 297 (1973).

[4] (a) M. H. Cohen and J. Lekner, Phys. Rev. **158**, 305 (1967); (b) S. Basak and M. H. Cohen, Phys. Rev. B **20**, 3404 (1979).

[5] S. Watanabe, J. Phys. Soc. Jpn. **49**, 38 (1980).

[6] V. M. Atrazhez and I. T. Iakubov, J. Phys. C **14**, 5139 (1981).

[7] A. Leycuras and J. Larour, J. Phys. C **15**, 6765 (1982).

[8] E. M. Gushchin, A. A. Kruglov, and I. M. Obodovskii, Zh. Eksp. Teor. Fiz. **B2**, 1114 (1982) [Sov. Phys.—JETP **55**, 650 (1982)].

[9] R. Reininger, U. Asaf, I. T. Steinberger, and S. Basak, Phys. Rev. B **28**, 4426 (1983).

[10] A. Vertes, J. Phys. Chem. **88**, 3722 (1984).

[11] J. K. Baird, Phys. Rev. A **32**, 1235 (1985).

[12] J. A. Jahnke, L. Meyer, and S. A. Rice, Phys. Rev. A **3**, 734 (1971).

[13] S. S.-S. Huang and G. R. Freeman, Phys. Rev. A **24**, 714 (1981).

[14] S. S.-S. Huang and G. R. Freeman, J. Chem. Phys. **68**, 1355 (1978).

[15] L. S. Miller, S. Howe, and W. E. Spear, Phys. Rev. **166**, 871 (1968).

[16] K. Yoshino, U. Sowada, and W. F. Schmidt, Phys. Rev. A **14**, 438 (1976).

[17] H. Schnyders, S. A. Rice, and L. Meyer, Phys. Rev. **150**, 127 (1966).

[18] J.-P. Dodelet and G. R. Freeman, Can. J. Chem. **55**, 2264 (1977).

[19] F. M. Jacobsen and G. R. Freeman, J. Chem. Phys. **84**, 3396 (1986).

[20] (a) W. B. Streett and L. A. K. Staveley, J. Chem. Phys. **55**, 2495 (1971); (b) W. B. Streett, L. S. Sagen, and L. A. K. Staveley, J. Chem. Thermodynam. **5**, 633 (1973); (c) D. L. Losee and R. O. Simmons, Phys. Rev. **172**, 944 (1968).

[21] N. B. Vargaftik, *Tables on the Thermophysical Properties of Liquids and Gases*, 2nd ed. (Wiley, New York, 1975), p. 575.

[22] R. A. Aziz, D. H. Bowman, and C. C. Lim, Can. J. Chem. **45**, 2079 (1967).

[23] (a) J. A. Cowan and J. W. Leech, Can. J. Phys. **61**, 895 (1983); (b) J. L. Kline and E. F. Carome, J. Chem. Phys. **58**, 4962 (1973).

[24] *Argon, Helium and The Rare Gases*, edited by G. A. Cook (Interscience, New York, 1961), Vol. 1, p. 360.

[25] M. A. Floriano and G. R. Freeman, J. Chem. Phys. (to be published).

[26] (a) B. V. Paranjape, Phys. Rev. A **21**, 405 (1980); (b) P. V. Panat, B. V. Paranjape, and R. Teshima, J. Phys. D **16**, 1477 (1983).

[27] R. E. Robson and E. A. Mason, Phys. Rev. A **25**, 2411 (1982).

[28] J. L. Pack, R. E. Voshall, and A. V. Phelps, Phys. Rev. **127**, 2084 (1962).

[29] E. Hausmann and E. P. Slack, *Physics* (Van Nostrand, New York, 1944), p. 412.

[30] N. Gee and G. R. Freeman, Phys. Rev. A **20**, 1152 (1979); **22**, 301 (1980).

[31] L. S. Frost and A. V. Phelps, Phys. Rev. **136**, A1538 (1964).

[32] N. Gee and G. R. Freeman, Can. J. Chem. (to be published).

[33] J. K. Baird, Phys. Rev. A **32**, 1235 (1985).

[34] J. K. Baird, J. Phys. Chem. **79**, 2862 (1975).

[35] A. C. Sinnock, J. Phys. C **13**, 2375 (1980).

[36] T. F. O'Malley, Phys. Rev. **130**, 1020 (1963).

[37] J. R. Reitz, F. J. Milford, and R. W. Christy, *Foundations of Electromagnetic Theory*, 3rd ed. (Addison-Wesley, Reading, Mass., 1979), Chaps. 2 and 4.